

Article

Mechanical Strength, Water Seepage and Microstructure of a Novel Landfill Solidified Sludge Liner Material

Yajun Liu ^{1,2}, Haijun Lu ^{1,2,*}, Chaofeng Wang ¹, Ye Liu ^{1,2}, Jiayu Ma ^{1,2} and Mengyi Liu ^{1,2}¹ School of Civil Engineering and Architecture, Wuhan Polytechnic University, Wuhan 430023, China² State Key Laboratory of Geomechanics and Geotechnical Engineering, Institute of Rock and Soil Mechanics, Chinese Academy of Sciences, Wuhan 430071, China

* Correspondence: luhaijun111@163.com

Abstract: In order to prepare a novel landfill liner material, we used industrial calcium-containing waste (slag, fly ash, and desulfurized gypsum) to solidify municipal sludge. The mechanical and permeability properties of the solidified sludge material (SSM) were evaluated using straight shear, uniaxial compression, and permeability tests. The hydration products, microscopic morphology, and elemental composition of the SSM after the wet and dry cycles were analyzed using a combination of scanning electron microscopy (SEM + EDS), X-ray diffraction (XRD), and Fourier transform infrared spectroscopy (FT-IR). The SSM has high strength and low hydraulic conductivity. The values of cohesion c and internal friction angle φ reached 0.45–3.31 MPa and 6.52–36.28°. The SSM exhibited a compressive strength of 0.93–11.67 MPa and hydraulic conductivity of 4.80×10^{-9} – 1.34×10^{-7} cm/s. Analysis shows that SiO₂, Al₂O₃, and CaO in industrial calcium-containing solid wastes and sludges produce dense bulk and agglomerated C-S-H and C-A-S-H gels under alkali excitation. The optimum ratio of sludge, desulfurized gypsum, fly ash, and slag in the solidified sludge was 1:0.61:0.62:0.54, whereas the optimum exciter was Ca(OH)₂. The SSM may be used as a good barrier material to prevent water seepage in landfills.



Citation: Liu, Y.; Lu, H.; Wang, C.; Liu, Y.; Ma, J.; Liu, M. Mechanical Strength, Water Seepage and Microstructure of a Novel Landfill Solidified Sludge Liner Material. *Processes* **2022**, *10*, 1641. <https://doi.org/10.3390/pr10081641>

Academic Editor: Adam Smoliński

Received: 15 July 2022

Accepted: 16 August 2022

Published: 18 August 2022

Publisher's Note: MDPI stays neutral with regard to jurisdictional claims in published maps and institutional affiliations.



Copyright: © 2022 by the authors. Licensee MDPI, Basel, Switzerland. This article is an open access article distributed under the terms and conditions of the Creative Commons Attribution (CC BY) license (<https://creativecommons.org/licenses/by/4.0/>).

Keywords: solidified sludge; landfill liner; industrial solid waste; water seepage; microstructure

1. Introduction

Currently, China's municipal sludge production exceeds 6×10^8 t/a [1], with an annual growth rate exceeding 18%. Sludge has a water content of 60–80% and contains a large number of pathogenic bacteria, parasites, heavy metals, and other harmful substances [2]. If inappropriately applied, sludge can trigger secondary pollution and damage ecosystems; therefore, finding a low-carbon and economical method for the environmentally sound treatment and utilization of sludge has become a priority. It was estimated that approximately 235 million tons of municipal solid waste were generated in China in 2021, and 500 million tons or more might be generated annually by 2050 [3,4]. The three main methods of waste disposal are sanitary landfills, incineration, and composting, with sanitary landfills accounting for 70% of waste disposal. The movement of leachate from sanitary landfills into the underlying soil and groundwater results in the release of many organic pollutants, heavy metal ions, and other toxic and harmful substances into the environment [5–7].

The liner impermeability system is an important part of the landfill ecological barrier system. It plays a vital role in preventing landfill leachate from contaminating groundwater and surface water. Its safety is also a key factor in ensuring the service performance of the landfill. Impermeable material systems commonly used as leachate barriers at landfills include compacted clay liners (CCL), geosynthetic clay liners (GCL), and high-density polyethylene (HDPE). The depth of solid waste at some landfills exceeds 100 m, and the corresponding pool of leachate can be tens of meters deep, which exerts immense pressure

on the landfill liner. Landfill leachate and groundwater can trigger the water absorption and humidification of CCL and GCL materials. Moreover, the temperature inside a landfill can be as high as 70 °C, with the corresponding temperature at the liner and sealing barrier as high as 50 °C [8]. Such high temperatures lead to critical levels of water loss and drying of CCL or GCL materials. High loads and dry–wet cycles ultimately trigger deformation and cracking of CCL as well as tearing of HDPE geomembranes and GCL; such damage to the liner results in the escape of leachate from the barrier system. To solve this problem, the research and development of a landfill liner barrier material with a high load-bearing capacity and durability has recently gained widespread attention from many researchers worldwide [9,10].

The dye sludge char has been previously treated with cement, lime, ladle slag, or hydroxyapatite for solidification and stabilization. The study showed that the unconfined compressive strength and permeability coefficient test results of the solidified sludge met the requirements for landfill cover material [11]. In previous studies of alkali slag–slag–lime solidified sludge, tests were performed to gauge the level of unconfined compression, variable head infiltration, water holding, and water resistance, as well as the strength characteristics and micromechanics of the sludge under dry–wet cycles. The unconfined compressive strength of the solidified sludge increased with the number of dry–wet cycles. Although the strength of the material slightly decreased after the first wet and dry cycles, after seven cycles, the strength of the samples was found to be 1.16–1.45 times higher than that before the dry–wet cycles. The results demonstrated that the unconfined compressive strength and permeability coefficient met the requirements for landfill cover materials [12,13]. Changjutturas et al. studied the geotechnical engineering properties such as unconfined compressive strength and microscopic pore structure of solidified sludge with fly ash geopolymers as a curing agent [14]. Li used sludge, cement, quicklime, and waste fly ash to solidify the municipal sludge and analyzed the strength and permeability of the solidified sludge under dry and wet cycles [15]. Yi et al. used quicklime or slaked lime mixed with slag, respectively, to solidify the soft clay. The research showed that the unconfined compressive strength of quicklime–slag solidified soft clay was higher than that of slaked lime–slag solidified soft clay at curing ages of 7 d and 28 d. However, the results for the unconfined compressive strength at 90 d were the opposite of those at 7 d and 28 d [16]. Furthermore, the sludge was solidified with cement and mineral powder, and the strength and heavy metal concentration of the solidified sludge were analyzed by orthogonal test. The study showed that when the solidifying agent content reached 15%, the compressive strength of the solidified sludge reached 1 MPa, and the leaching concentration of heavy metal ions met the standard requirements [17]. Numerous researchers used clay, lime, fly ash, and ferric chloride as the curing agent to solidify the sludge. They tested unconstrained compressive strength, shear strength, coefficient of permeability, expansion and contraction, and contaminant concentration of solidified sludge. The results revealed that it could be used as an alternative material for landfill protection [18–21]. Furthermore, Bizarreta et al. examined the mineralogical and morphological characteristics of sludge as a leachate barrier. The authors performed shrinkage tests on selected sludge samples with different moisture contents and assessed the potential of sludge as a final cover material for partial landfills [22]. Yang et al. utilized an in-house curing agent to cure municipal sludge. The material was tested for unconsolidated undrained creep through different wet and dry cycles. The authors ultimately showed that the strength of the solidified sludge gradually decreased as the number of dry–wet cycles increased; when the number of wet and dry cycles exceeded 10, the strength remained constant [23].

The above studies mainly used cement, lime, and fly ash to solidify sludge as an impermeable material for landfills. Although the solidified sludge material (SSM) is characterized by low permeability, the bearing capacity of the material is rather low, and its durability against dry and wet cycles is weak. These problems have seriously affected the service performance of the impermeable system and caused great harm to the long-term safety of the landfill and the ecological environment. Currently, in China's industrial

solid waste overproduction, most of the industrial waste cannot be fully utilized. The solidification of sludge using industrial solid waste materials (slag, fly ash, and desulfurized gypsum) and its application as a landfill liner barrier material are less studied. Therefore, curing sludge with slag, fly ash, and desulfurization gypsum to obtain a novel landfill liner barrier material.

In the present study, industrial solid waste calcium-containing wastes (slag, fly ash, and desulfurized gypsum) were utilized as modifiers of municipal sludge to be solidified under alkaline excitation conditions to obtain landfill liner material. The optimum ratio of the SSM and the optimum type and content of alkali excitation were selected using a response surface test design and a single-factor controlled test design. The mechanical characteristics and impermeability of the solidified sludge were evaluated using shear, uniaxial compressive, and permeability tests. The solidified sludge was immersed in the solution (pH = 7.00) for 270 d, and the heavy metal concentrations in the solutions were measured using a portable pH meter and an atomic emission spectrometer. Furthermore, X-ray diffraction (XRD), Fourier transform infrared spectroscopy (FT-IR), and scanning electron microscopy (SEM + EDS) experiments were conducted to examine the hydration products, microscopic morphology, and elemental composition of the solidified sludge during different drying and wetting cycles. Based on these analyses, we confirmed the solidification of sludge using industrial calcium-containing solid waste and discovered the microscopic mechanism of the damage caused by dry–wet cycles to the solidified sludge structure.

2. Materials and Test Methods

2.1. Materials

2.1.1. Raw Materials

The municipal sludge used in the experiment was obtained from a sewage treatment plant in the suburbs of Wuhan. It was characterized by a dark brown appearance with an initial moisture content of 75–85%. Desulfurization gypsum was a secondary product of flue gas desulfurization gypsum in the form of a white powder. The fly ash was grade II gray–black powder. The slag powder was S95 grade, a gray–white powder with a particle size of 1–35 μm and a specific surface area of 430–460 m^2/kg . The chemical composition and contents of the test materials are summarized in Table 1.

Table 1. Chemical composition and content of test materials.

Name of Raw Material	Main Chemical Composition/%							
	SiO ₂	Al ₂ O ₃	Fe ₂ O ₃	CaO	MgO	K ₂ O	Na ₂ O	Others
Desulfurization gypsum	31.89	12.45	0.56	31.37	7.61	0.59	0.51	15.02
Fly ash	47.17	27.15	4.89	3.54	0.38	1.39	0.68	14.80
Slag powder	29.73	13.58	1.01	36.39	6.56	0.55	0.28	11.90
Municipal sludge	39.46	11.10	7.00	3.96	1.80	2.36	0.70	33.62

2.1.2. Samples Molding

A cement mortar mixer (JJ-5, Wuxi Jianding Construction Instrument Factory, Wuxi, China) was used to stir the municipal sludge at a low speed of 100–400 rpm for 5–10 min to achieve a viscous consistency. Subsequently, desulfurized gypsum, fly ash, and slag powder were successively added to the mixing pot and mixed at a high speed of 600–1000 rpm for 10–20 min, followed by the addition of 0.2–2% of an activator (Na₂SiO₃, Na₂CO₃, Na₂SO₄, Ca(OH)₂, and NaOH). The contents were thoroughly mixed and pressed into a cylindrical mold (100 mm in height and 50 mm in diameter) to prepare a solidified sludge specimen. The ratio of test materials was designed using the central composite design method (CCD) in RSM. Samples MS1–MS15 were prepared using this ratio. The uniaxial compressive strength was considered as the main index. The optimal ratio of the solidified material to the activator was selected to prepare the MS16 sample. Furthermore, 2% Ca(OH)₂ was

added to prepare MS17 and MS18 samples based on the material ratios of MS4 and MS9. The material ratios of the MS1–MS18 samples are summarized in Table 2.

Table 2. Material composition of MS1–MS18 samples (g).

Serial Number	Desulfurized Gypsum	Fly Ash	Slag Powder	Municipal Dewatered Sludge	Ca(OH) ₂
MS1	27.5	27.5	27.5	50	/
MS2	15	40	40	50	/
MS3	40	15	15	50	/
MS4	40	40	15	50	/
MS5	15	15	40	50	/
MS6	15	15	15	50	/
MS7	15	40	15	50	/
MS8	40	15	40	50	/
MS9	40	40	40	50	/
MS10	6.48	27.5	27.5	50	/
MS11	27.5	27.5	6.48	50	/
MS12	48.52	27.5	27.5	50	/
MS13	27.5	48.52	27.5	50	/
MS14	27.5	27.5	48.52	50	/
MS15	27.5	6.48	27.5	50	/
MS16	30.47	31.14	27.15	50	2.77
MS17	40	40	15	50	2.90
MS18	40	40	40	50	3.40

2.2. Methods

2.2.1. Uniaxial Compressive Strength and Shear Strength Tests

The uniaxial compressive strength of the solidified sludge sample after curing for 28 d was measured using a microcomputer-controlled electronic rock shearing instrument (YZW-30A, Jinan Puye Electromechanical Technology Co., Ltd., Jinan, China). The samples were cylinders with a height of 100 mm and a diameter of 50 mm. A stress-controlled axial load was applied in the uniaxial compressive test at a loading rate of 0.01 KN/s.

After curing for 28 d, the MS16–MS18 samples were placed indoors and immersed in distilled water for 30, 90, 180, and 270 d. The shear and uniaxial compressive strengths of the samples were tested using straight rock shear. The shear strength test was set at a vertical loading rate of 0.01 MPa/s, with limits of 0.5, 1.0, 1.5, 2.0, and 2.5 MPa and a horizontal displacement of 0.01 mm/s.

2.2.2. Permeation Test

Permeation tests of samples were performed using an environmental geotechnical flexible wall permeameter (PN3230M, GEOEQUIP, Boston, MA, USA) following the American experimental standard ASTM (D5084-03). In the test, the confining pressure was set to 350 KPa, whereas the upper and lower back pressures were 30 and 60 KPa, respectively. Before the penetration test, the sample was vacuum-saturated for 24 h with distilled water as the saturated medium.

2.2.3. Dry-Wet Cycle Test

The uniaxial compressive strength and hydraulic conductivity of MS16–MS18 solidified sludge samples were tested during repeated wet and dry cycles after 28 d of maintenance to evaluate the service performance of the SSM under the action of wet and dry cycles. The samples were placed in a DHG-9071A type constant temperature drying oven (Shanghai Yiheng Technology Instruments Co., Ltd., Shanghai, China) at a constant temperature of 50 °C for 24 h. Then, dried samples were placed in a BGH vacuum-saturated cylinder for 24 h. This process accounted for one dry–wet cycle. The number of dry–wet cycles for this test was 1–10.

2.2.4. Toxicity Leach Test

After 270 d of samples immersion, heavy metal concentrations in the immersion solution (pH = 7.00) were measured using a portable pH meter and an atomic emission spectrometer (Agilent 725-ES, Agilent Corporation, Palo Alto, CA, USA).

2.2.5. Micromechanic Test

After curing for 28 d and undergoing 1, 3, and 5 dry/wet cycles, MS16 samples were selected and comprehensively analyzed using XRD (D8Advance, Bruker Corporation, Karlsruhe, Baden-Württemberg, Germany), FT-IR (Nicolet6700, Thermo Fisher Scientific, Waltham, MA, USA), and SEM (Gemini SEM 300, Carl Zeiss AG, Jena, Germany) to detect the hydration products, microscopic morphology, and elemental composition of the solidified sludge.

3. Results and Discussions

3.1. Uniaxial Compressive Strength and Shear Strength

During the curing of industrial solid waste-solidified sludge, the hydration reaction contributes to the strength of the sludge. Figure 1 shows that the uniaxial compressive strengths of the MS1–MS15 samples after curing for 28 d were 2.63–5.25 MPa. As the content of desulfurized gypsum, fly ash, and slag powder increased from 15 to 40%, the compressive strength first increased but then decreased, as shown in Figure 2. When less industrial solid waste material is added, the high water content of the modified sludge material is not conducive to early strength generation. When more mass was added, a complete hydration reaction did not occur. Moreover, the change in the mass ratio of the three materials resulted in a convex shape of the compressive strength response surface. The optimum ratio of the SSM was determined through ANOVA with a quadratic polynomial regression response surface model; it was 1/0.61/0.62/0.54 for fresh municipal sludge/desulfurized gypsum/coal ash/slag powder, respectively.

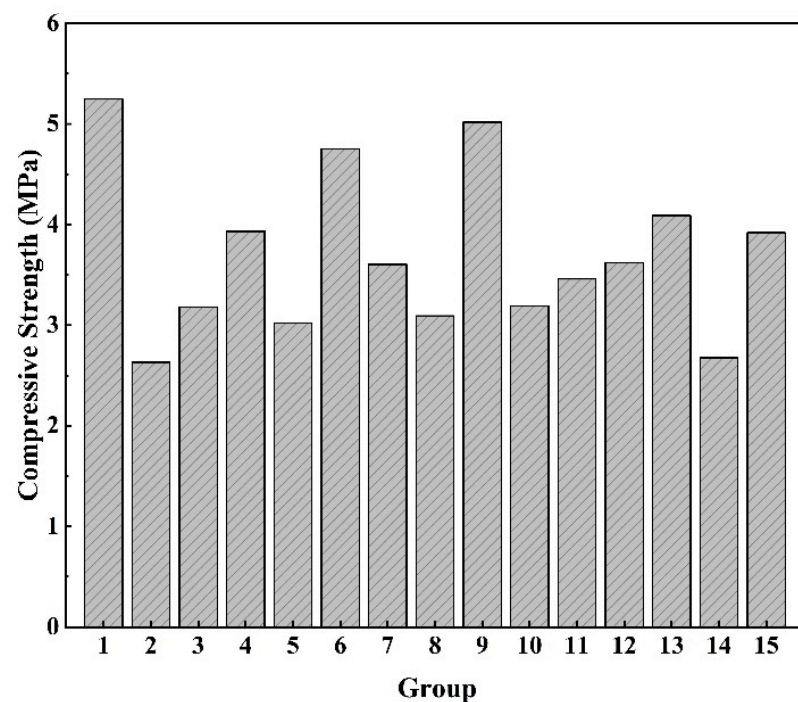
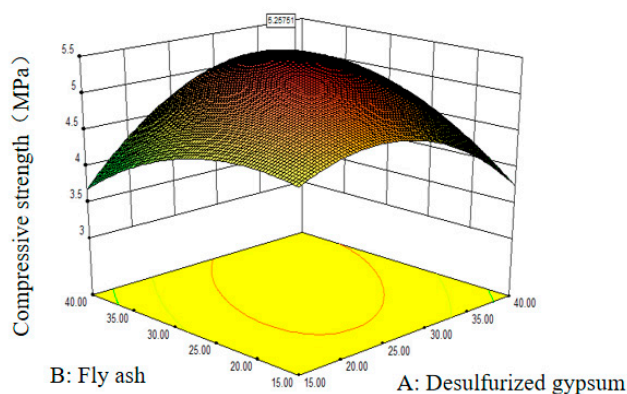
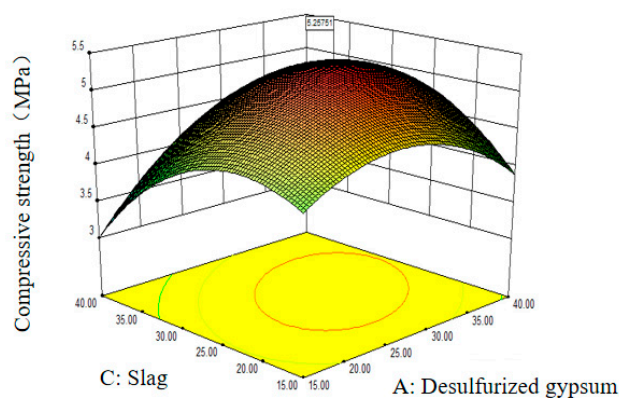


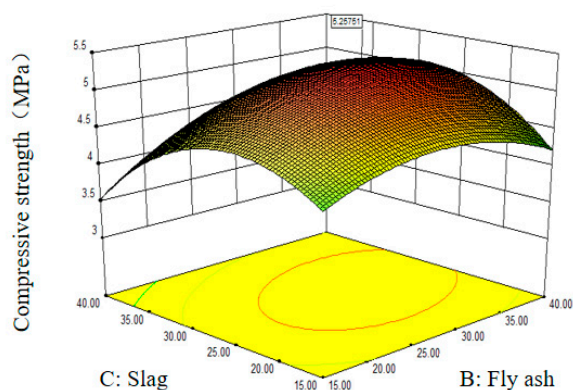
Figure 1. Compressive strength of MS1–MS15 samples.



(a)



(b)



(c)

Figure 2. Response surface analysis results of different materials. (a) Desulfurized gypsum and fly ash. (b) Desulfurized gypsum and slag powder. (c) Fly ash and slag powder.

Figure 3 shows the compressive strengths of the solidified sludge samples prepared with the optimum material ratios and activator types and levels. The compressive strength of the solidified sludge under the action of sodium salts (e.g., Na_2SiO_3 , Na_2CO_3 , and Na_2SO_4) first increased but then decreased. Overall, sodium salts only slightly enhanced the strength of the solidified sludge. With the addition of alkali ($\text{Ca}(\text{OH})_2$, NaOH), the

compressive strength of the solidified sludge increased significantly, and the $\text{Ca}(\text{OH})_2$ alkali activator exhibited the most significant effect. At a $\text{Ca}(\text{OH})_2$ content of 2.0%, the compressive strength of the solidified sludge reached 15.23 MPa at 28 d curing age, which was twofold higher than the compressive strength of the solidified sludge without the addition of an alkali activator.

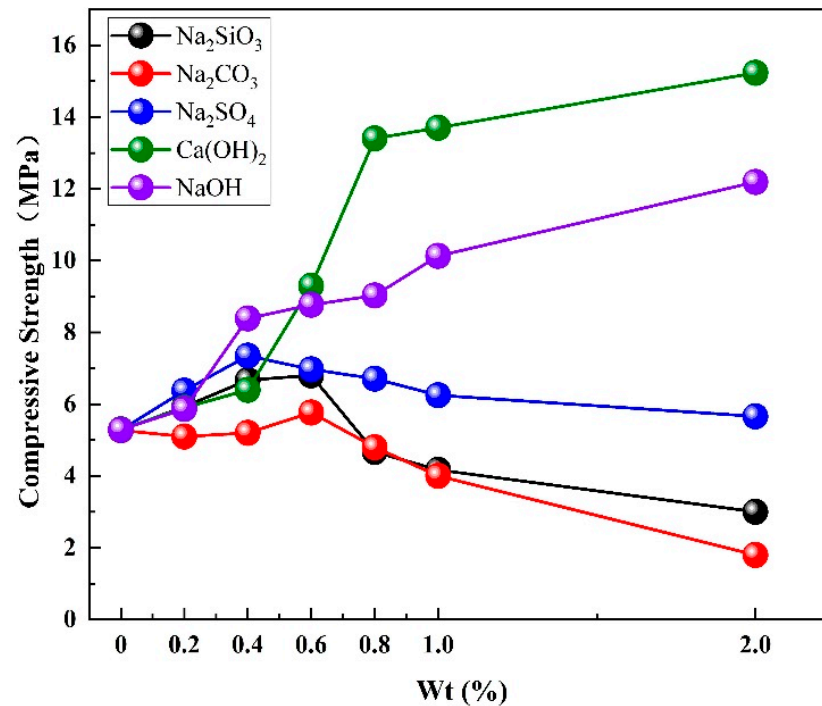
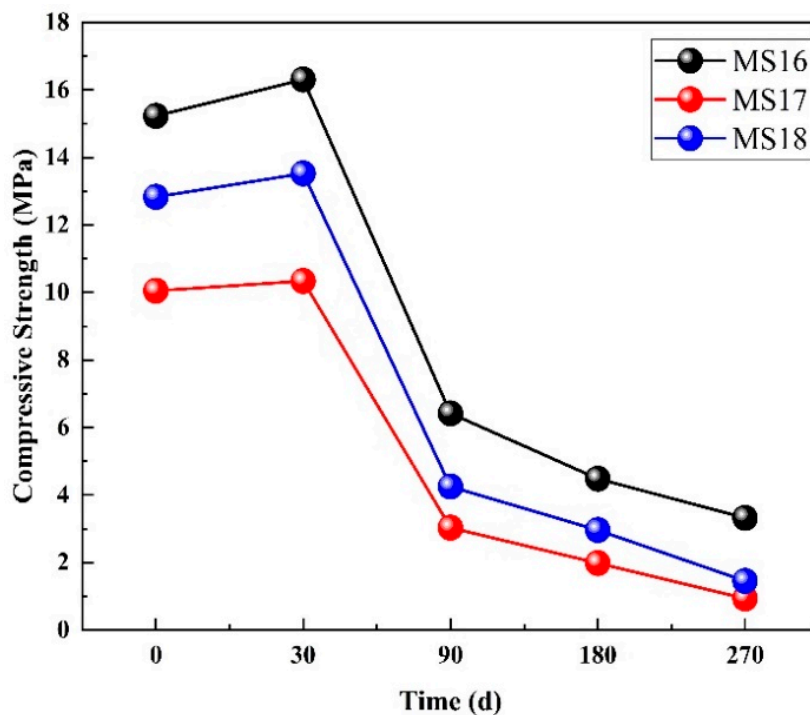


Figure 3. Compressive strength of solidified sludge samples with different additives.

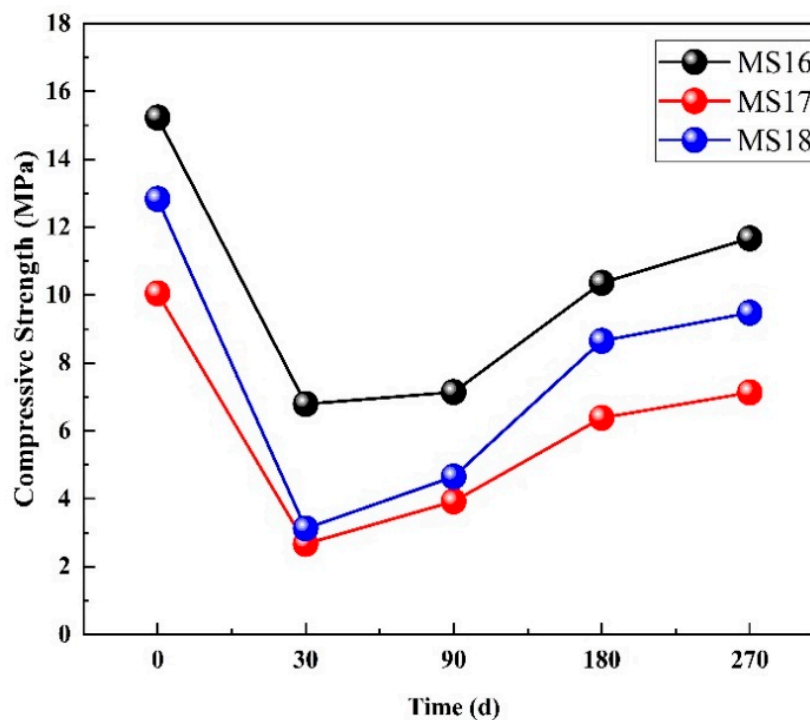
Figure 4 shows the uniaxial compressive strengths of the solidified sludge exposed to air and immersed in water. As shown, the compressive strength of MS16–MS18 samples exhibited a complex trend by first slowly increasing and then rapidly decreasing with the prolongation of exposure time in the air, whereas it first decreased rapidly and then slowly increased with the prolongation of water immersion time. After the exposure to air or immersion in water for 30 d, the compressive strength of the samples increased from 10.05–15.23 MPa to 10.34–16.31 MPa or decreased to 2.67–6.79 MPa. After being exposed to air or immersed in water for 30–270 d, the compressive strength consistently decreased to 0.93–3.32 MPa or increased to 7.13–11.67 MPa, respectively. The maximum compressive strength was observed for the MS16 specimen. The solidified sludge was exposed to air for a long time to cause water loss, which resulted in structural damage and loosened the contact of the particles, ultimately weakening the strength. When soaked in water, industrial calcium-containing solid waste can generally continue to undergo hydration reactions, thus facilitating the construction of the skeletal structure and promoting increased strength. These findings suggest that solidified sludge is potentially efficient for landfill liner barriers and can maintain a high load-bearing capacity when immersed in water.

Figure 5a shows that the cohesion (c) and internal friction angle (φ) of MS16–MS18 samples exposed to air and immersed in water exhibited similar evolutionary patterns to the compressive strength. In particular, c increased from 1.83–3.15 MPa to 1.93–3.31 MPa, while φ increased from 16.05–27.57° to 17.97–36.28° after 30-day exposure to air. After 30–270 d of exposure to air, c and φ both rapidly decreased to 0.45–0.90 MPa and 6.52–11.23°, respectively. Figure 5b illustrates that both c and φ of the MS16–MS18 samples exhibited a trend of rapid decrease, followed by a slow growth with increasing water immersion time. When samples were immersed in water for 0–30 d, c and φ both decreased from 1.83–3.15 MPa and 16.05–27.57° to 0.64–1.98 MPa and 9.75–17.88°, respectively. When the samples were

immersed in water for 30–270 d, c and φ , both slowly increased to 0.96–2.75 MPa and 11.32–19.94°, respectively. The MS16 sample exhibited the maximum shear strength.



(a)



(b)

Figure 4. Compressive strength of MS16–MS18 samples exposed to air or immersed in water. (a) Exposed to air. (b) Immersed in water.

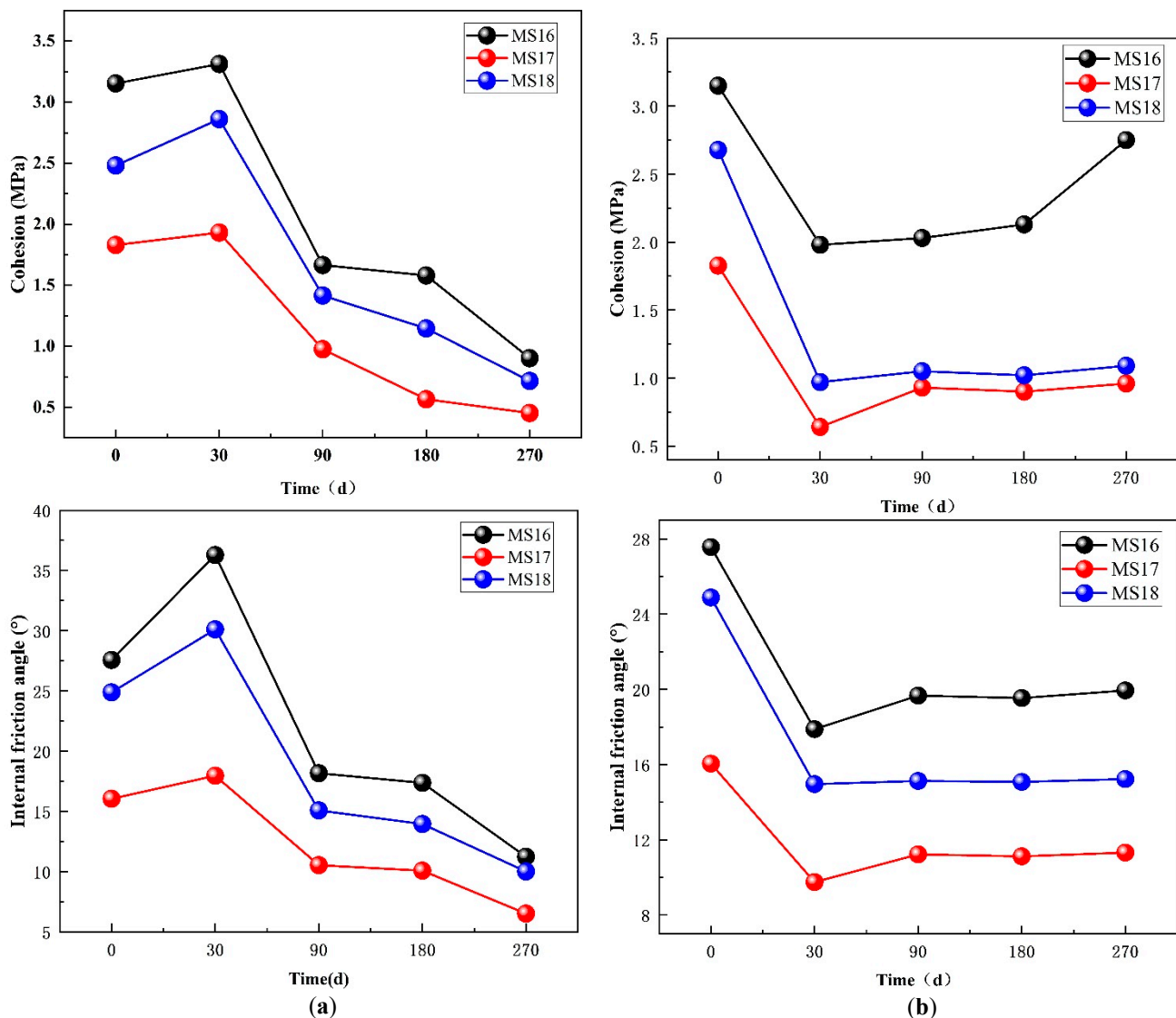


Figure 5. The internal friction angle and cohesion of MS16–MS18 samples exposed to air or immersed in water. (a) Exposed to air. (b) Immersed in water.

Ca^{2+} , Al^{3+} , SiO_4^{4-} , and SO_4^{2-} ions in desulfurization gypsum, fly ash, slag powder, and municipal sludge generated C-S-H and ettringite in a $\text{Ca}(\text{OH})_2$ alkaline environment, thus filling the material pores and making the SSM denser. Furthermore, this made the specimen mechanically stronger when it was exposed to air. Moreover, as the exposure time to air increased, the moisture content in the solidified sludge decreased, and the hydration reaction between the materials was slow. In a dry environment, ettringite generally reacts with CO_2 in the air, and part of the ettringite is converted into a powder form of gypsum and vaterite [24], thereby inducing a decrease in the ettringite content in the solidified sludge and a decrease in the mechanical strength. At the initial stage of immersion in water, hydration products such as ettringite in the solidified sludge expanded when exposed to water; while the skeleton structure was destroyed, the pore size increased, and the strength decreased. As the soaking time in water increased, some substances, such as desulfurized gypsum, fly ash, and slag powder, underwent hydration reactions with water once again to generate ettringite and C-S-H cementitious substances, resulting in increased strength.

3.2. Hydraulic Conductivity

Figure 6 shows the hydraulic conductivities of the MS16–MS18 samples when exposed to air or immersed in water. As shown in Figure 6a, the hydraulic conductivity of MS16–MS18 exhibited a tendency to decrease or increase first with increasing exposure time. The hydraulic conductivity decreased from 7.70×10^{-9} – 4.33×10^{-8} cm/s to 4.30×10^{-9} – 3.53×10^{-8} cm/s in the first 30 d. After 270 d of exposure, the hydraulic conductivity increased up to 1.25×10^{-8} – 5.54×10^{-8} cm/s. Moreover, Figure 6b demonstrates that the hydraulic conductivity rapidly increased from 7.70×10^{-9} – 4.33×10^{-8} cm/s up to 1.59×10^{-8} – 5.77×10^{-8} cm/s after soaking for 0–30 d. After soaking for 30–270 d, the hydraulic conductivity slowly decreased to 4.80×10^{-9} – 4.54×10^{-8} cm/s. Furthermore, the hydraulic conductivity coefficients of MS16, MS18, and MS17 are in descending order. Notably, they all met the impermeability requirements for landfill liner barriers of less than 1.0×10^{-7} cm/s. At the initial stage of water immersion, tiny particles and soluble filling in the pores of the material were lost during the dissolution of water, and the pores of the material increased, thereby increasing the permeability coefficient of the solidified sludge. As the soaking time increased, some of the material within the solidified sludge continued to undergo a hydration reaction, thereby generating gelling products that filled the pores, which ultimately reduced the permeability coefficient.

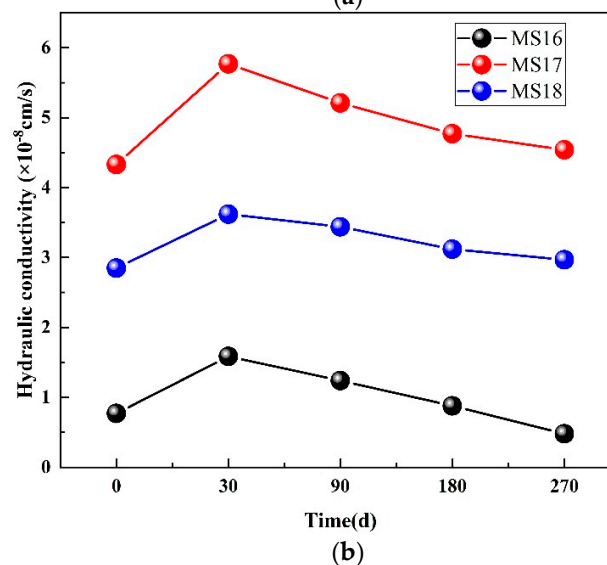
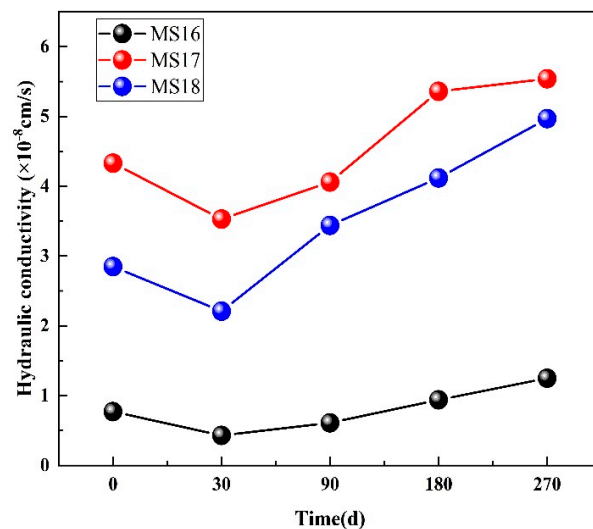


Figure 6. Hydraulic conductivity of MS16–MS18 samples exposed to air or immersed in water. (a) Exposed to air. (b) Immersed in water.

3.3. Service Characteristics during Dry–Wet Cycle

Figure 7 shows the compressive strength and hydraulic conductivity of the MS16–MS18 samples under dry and wet cycling conditions. As shown, the compressive strength and hydraulic conductivity continued to change with the number of wet and dry cycles. When the number of dry-wetting cycles was 0–5, the compressive strength of the MS16–MS18 samples rapidly decreased from 9.92–15.23 MPa to 4.05–7.86 Mpa, and the hydraulic conductivity increased from 2.59×10^{-8} – 6.28×10^{-8} cm/s up to 8.62×10^{-8} – 1.30×10^{-7} cm/s. After five wet cycles, the compressive strength and hydraulic conductivity of the samples stabilized. After 10 wet and dry cycles, the compressive strength and hydraulic conductivity reached 3.74–7.54 MPa or 8.96×10^{-8} – 1.34×10^{-7} cm/s, respectively. These findings indicate that the dry–wet cycle inflicted a damaging effect on the structure of the solidified sludge. After multiple drying and wetting cycles, the compressive strength of the solidified sludge could still withstand a pressure of hundreds of meters of landfill waste, but only the hydraulic conductivity of the MS16 sample was below 1.0×10^{-7} cm/s. Therefore, it is reasonable to suggest that MS16 is a beneficial, durable barrier material for landfill liners. During the drying and wetting process, the partially bound water of the solidified sludge was separated from the mineral particles, the material structure was destroyed, and tiny pores developed into mesopores or macropores. The ettringite generated by the hydration reaction expanded during the drying–wetting cycle, resulting in pores between the particles inside the material.

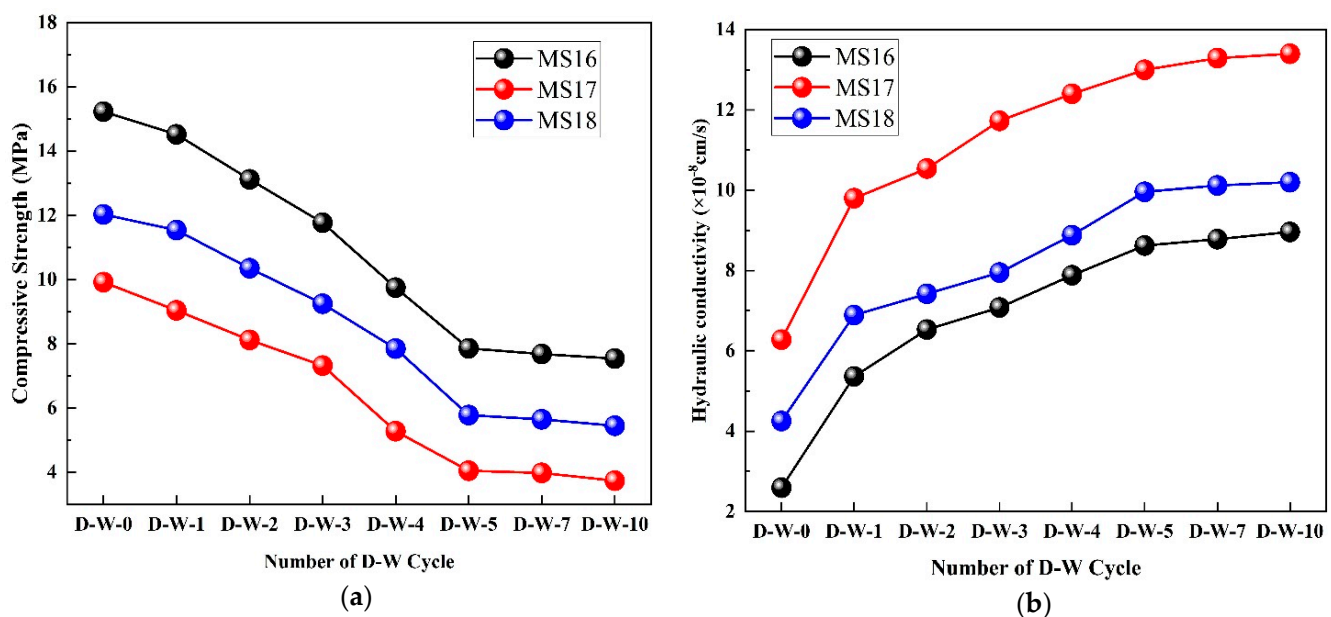


Figure 7. Compressive strength and hydraulic conductivity of MS16–MS18 samples during drying–wetting cycles. (a) Compressive strength; (b) Hydraulic conductivity.

3.4. Leaching Toxicity Element Analysis

After 270 d of MS16 sample immersion, elemental fractions in a solution (pH = 7.00) were examined to evaluate the ecological and environmental benefits of the impermeable layer of the modified sludge liner in long-term solutions. The results are presented in Table 3.

Table 3. Elemental composition of the solution (pH = 7.00) after 270 days of immersion.

Chemical Element	Content (mg/L)
S	1870.1250
Ca	768.1050
Na	598.3800
Mg	2.0083
Zn	0.0379
Fe	1.6736
Ni	0.4875
Ba	0.2143
Cr	0.1075
Se	0.0352
As	0.6942
Pb	0.0510
Cu	0.1754
Hg	0.0281
Ag	0.0349
Cd	0.0414
Be	0.0008

By comparing the concentrations of hazardous components in the solution, it was found that the actual concentrations of Cu, Zn, and Ba were 3–4 orders of magnitude lower than the normative limits; the concentrations of Cd, Pb, Cr, Be, Ni, Ag, As, and Se were 1–3 orders of magnitude lower. The concentration range of elemental Hg is 0.0077–0.0925 mg/L, also lower than the specification requirement limit of 0.1 mg/L. According to the Hazardous Waste Identification Standard Leaching Toxicity Identification (GB 5085.3-2019), standard limits for leaching toxic inorganic elements are required in the specification. This study found that the concentrations of all hazardous elements in the solution were 1–4 orders of magnitude lower than the normative limits, meeting the normative requirements. In summary, the SSM is believed to have a better environmental effect.

3.5. Micromechanics

Figure 8 shows the XRD pattern of the MS16 specimen during the wet and dry cycles. The main hydration products in the solidified sludge were ettringite ($\text{Ca}_6\text{Al}_2(\text{SO}_4)_3(\text{OH})_{12}\cdot 26\text{H}_2\text{O}$), calcium silicate hydrate (C-S-H), calcite (CaCO_3), and gypsum ($\text{CaSO}_4\cdot 0.5\text{H}_2\text{O}$ and $\text{CaSO}_4\cdot 2\text{H}_2\text{O}$). Moreover, Figure 8 reveals that large amounts of ettringite and small amounts of C-S-H gels were generated within the modified sludge when no wet–dry cycling was performed. As the number of dry and wet cycles increased, the peak value of $\text{Ca}_6\text{Al}_2(\text{SO}_4)_3(\text{OH})_{12}\cdot 26\text{H}_2\text{O}$ decreased, whereas those of $\text{CaSO}_4\cdot 2\text{H}_2\text{O}$ and CaCO_3 increased. The channel structure of ettringite accommodates sulfate, which is relatively easily replaced by oxoacid anions with a similar structure and radius [25]. Furthermore, alumite is decomposed into gypsum, vaterite, and alumina gel via a carbonization reaction, which destroys the internal structure of the material [26].

Figure 9 shows the FT-IR spectral profile of the MS16 specimen. The absorption peaks at positions 465.04^{-1} – 470.69^{-1} characterized the bending vibrations of Si-O-Si in C-S-H gels, while 1004.75^{-1} – 1014.39^{-1} and 1121.53^{-1} – 1148.63^{-1} most likely characterized the bending vibrations of Si-O in C-S-H gels. The absorption peaks at 3540.90^{-1} corresponded to the O-H stretching vibration absorption peak of $\text{Ca}(\text{OH})_2$, and the peaks at positions 875.06^{-1} and 1440.66^{-1} – 1450.49^{-1} are characteristic of the asymmetric stretching vibrations of carbonate C-O bonds. Combined with the XRD analysis, the hydration products mainly included ettringite, calcium silicate hydrate gel, and calcium carbonate. As the number of wet and dry cycles increased, the absorption peaks at 465.04^{-1} , 1004.75^{-1} , and 1121.09^{-1} shifted to 470.69^{-1} , 1014.39^{-1} , and 1148.63^{-1} , respectively. Note that the peak shifts to higher wavenumbers indicate an increase in the polymerization of silicon oxide tetrahedra in the gel products. Similarly, the absorption peak at 1140.66^{-1} shifted to 1450.49^{-1} ,

indicating that the degree of C-O polymerization also increased in the calcite [27]. This finding also indicates the production of small amounts of C-S-H gels and ettringite during the pre-dry and wet cycles.

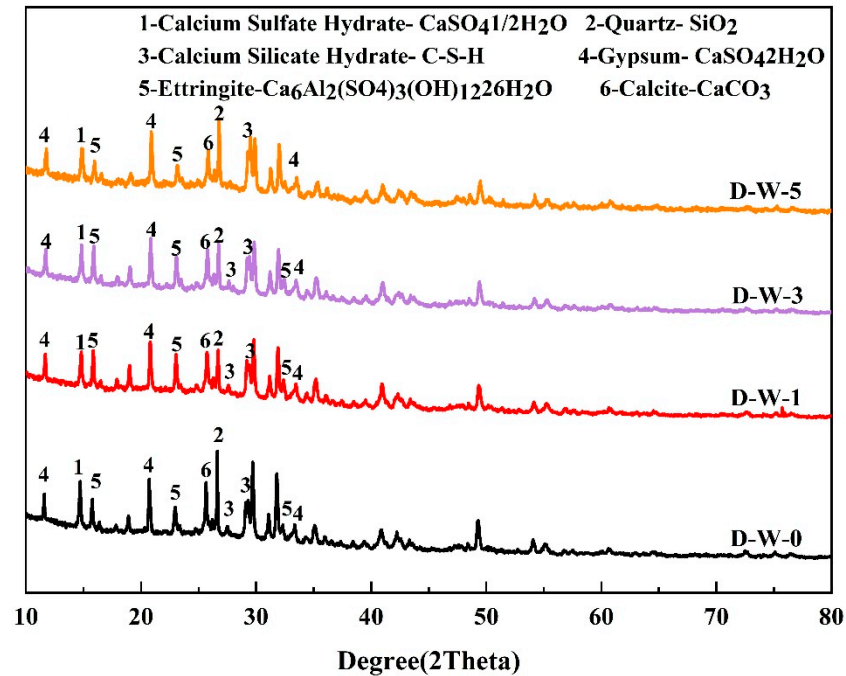


Figure 8. X-ray diffraction of MS16 sample.

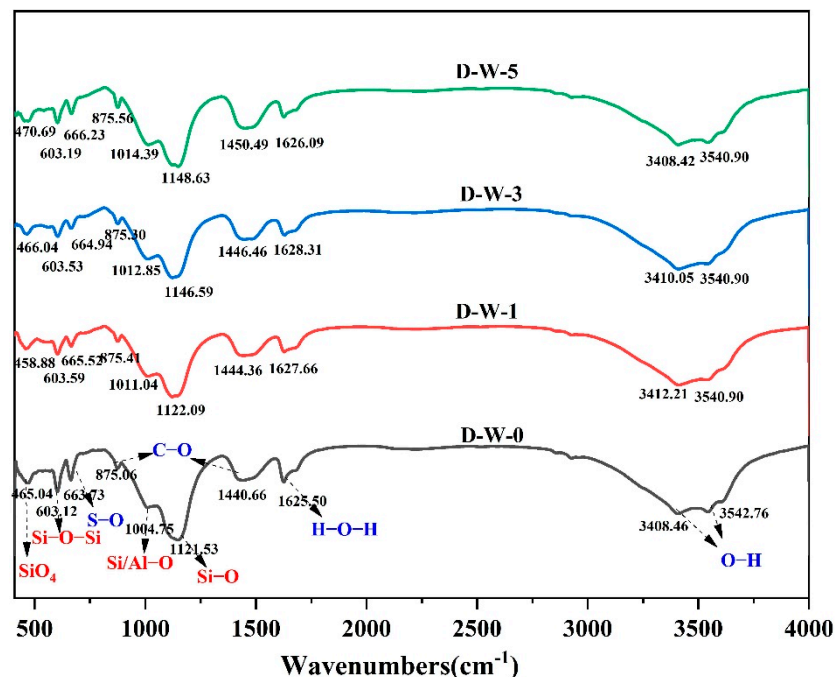


Figure 9. The FT-IR spectra of MS16 sample.

Figure 10 shows the surface micromorphology and elemental composition of MS16 during wet and dry cycles. The surfaces of the samples without wet and dry cycles appeared as lumps, rods, and flocculent colloidal material stacked on top of each other, with larger spherical fly ash particles covered by rods and flocculent colloidal material, as well as fine fissures and pores of different sizes. However, as the number of wet and

dry cycles increased, the hydration products shrank owing to water loss and expanded owing to water absorption, thereby triggering the emergence of more cracks and larger pores. Spherical fly ash particles were damaged by erosion and gradually decreased in size. The material composition and XRD pattern analysis indicated that the dense masses and flocculent colloids were mainly composed of hydrated C-S-H gels, and the rods were mainly composed of structural crystals of ettringite and calcite. Furthermore, EDS results demonstrated that the main elements of the solidified sludge hydration products were O, Si, Al, and Ca, with only a small amount of S. The Ca/Si ratio ranged between 0.8 and 1.5, thereby proving the formation of C-S-H gels and ettringite in the modified sludge.

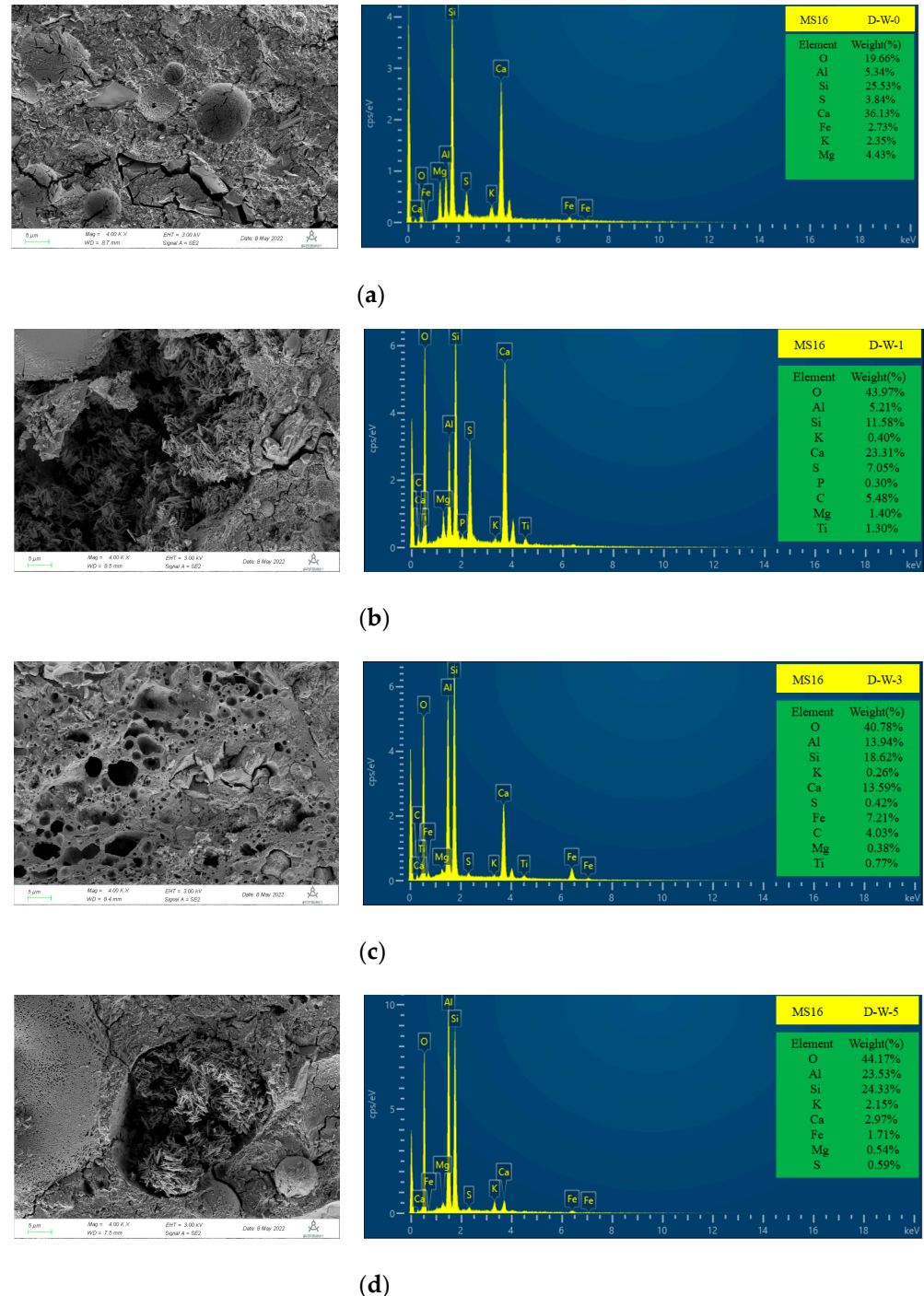


Figure 10. The SEM and EDS semi-quantitative spectrogram of MS16 sample. (a) D-W-0. (b) D-W-1. (c) D-W-3. (d) D-W-5.

4. Conclusions

In this study, a novel type of impermeable barrier material for landfill liners was prepared using industrial calcium-containing waste (slag, fly ash, and desulfurized gypsum) to solidify municipal dewatered sludge. The load-bearing capacity and impermeability of solidified sludge under long-term exposure to air, immersion in water, and repeated wet and dry cycles were systematically evaluated. This study described the solidification of sludge with calcium-containing solid waste and the microscopic mechanism of structural damage caused by dry–wet cycles to the solidified sludge. The optimum ratio of sludge, desulfurized gypsum, fly ash, and slag in the solidified sludge was 1:0.61:0.62:0.54, whereas the optimum exciter was $\text{Ca}(\text{OH})_2$. After 270 d of exposure to air or immersion in water, the solidified sludge exhibited a compressive strength of 0.93–3.32 MPa or 7.13–11.67 MPa and a hydraulic conductivity of 1.25×10^{-8} – 5.54×10^{-8} cm/s or 4.80×10^{-9} – 4.54×10^{-8} cm/s. After ten wet and dry cycles, the SSM reached the compressive strength of 3.74–7.54 MPa and hydraulic conductivity of 8.96×10^{-8} – 1.34×10^{-7} cm/s. The values of cohesion c and internal friction angle φ of the SSM reached 0.45–0.90 MPa and 6.52 – 11.23° or 0.96–2.75 MPa and 11.32 – 19.94° . The MS16 sample met the anti-seepage requirements of the landfill liner impermeability system with a high load-bearing capacity. This is because O, Si, Al, and Ca in industrial calcium-containing solid waste and sludge generate dense blocks and agglomerated C-S-H and C-A-S-H gels in the presence of alkali excitation. Under the action of dry and wet cycles, the calcium alumina in the solidified sludge was converted into gypsum and calcium carbonate. At the same time, some of the hydration products expanded and contracted, resulting in the destruction of the skeletal structure and an increase in pores and cracks. However, the compressive strength and permeability coefficient of the solidified sludge still met the impermeability requirements of landfill liners. The heavy metal content in the solution of the MS16 sample was less than the specification after 270 d of immersion in the solution (pH = 7.00). In summary, solidified municipal sludge with calcium-containing waste (slag, fly ash, and desulfurized gypsum) can serve as a landfill liner impermeable material.

Author Contributions: Conceptualization, H.L.; Data curation, Y.L. (Yajun Liu) and Y.L. (Ye Liu); Formal analysis, Y.L. (Yajun Liu); Investigation, Y.L. (Yajun Liu); Methodology, H.L.; Project administration, J.M.; Resources, M.L.; Software, C.W.; Visualization, C.W.; Writing—original draft, Y.L. (Yajun Liu); Writing—review & editing, H.L. All authors have read and agreed to the published version of the manuscript.

Funding: This research was funded by National Natural Science Foundation of China (U20A20320).

Institutional Review Board Statement: Not applicable.

Informed Consent Statement: Not applicable.

Data Availability Statement: Data is contained within the article.

Conflicts of Interest: The authors declare no conflict of interest.

References

1. Xie, K.; Yin, J.; Chen, X. Research progress on sludge treatment technology of urban sewage treatment project in China. *Ind. Water Treat.* **2020**, *40*, 18–23.
2. Fu, K.M.; Liao, M.H.; Wang, J.; Yang, Z.M.; Li, H.; Qiu, F.G. Present situation on low concentration domestic wastewater in villages and towns and its treatment technology analysis. *Environ. Eng.* **2019**, *37*, 5.
3. Qin, G.W. Brief Introduction and Processing Technologies of Landfill Leachate. *Guangdong Chem. Ind.* **2018**, *45*, 2.
4. Wang, L.; Yan, D.; Xiong, Y.; Zhou, L. A review of the challenges and application of public-private partnership model in Chinese garbage disposal industry. *J. Clean. Prod.* **2019**, *230*, 219–229. [[CrossRef](#)]
5. McGrath, S.P.; Chaudri, A.M.; Giller, K.E. Long-term effects of metals in sewage sludge on soils, microorganisms and plants. *J. Ind. Microbiol.* **1995**, *14*, 94–104. [[CrossRef](#)] [[PubMed](#)]
6. Rezapour, S.; Samadi, A.; Kalavrouziotis, I.K.; Ghaemian, N. Impact of the uncontrolled leakage of leachate from a municipal solid waste landfill on soil in a cultivated-calcareous environment. *Waste Manag.* **2018**, *82*, 51–61. [[CrossRef](#)]
7. Szymański, K.; Janowska, B.; Izewska, A.; Sidelko, R.; Siebielska, I. Method of evaluating the impact of landfill leachate on groundwater quality. *Environ. Monit. Assess.* **2018**, *190*, 415. [[CrossRef](#)]

8. Klein, R.; Baumann, T.; Kahapka, E.; Niessner, R. Temperature development in a modern municipal solid waste incineration (MSWI) bottom ash landfill with regard to sustainable waste management. *J. Hazard. Mater.* **2001**, *83*, 265–280. [[CrossRef](#)]
9. Kiser, B. Getting the circulation going. *Nature* **2016**, *531*, 443–445.
10. Xue, Q.; Chen, Y.-J.; Liu, L. Erosion characteristics of ecological sludge evapotranspiration cover slopes for landfill closure. *Environ. Earth Sci.* **2016**, *75*, 419. [[CrossRef](#)]
11. Sanghwa, O.; Won, S.S. Applicability of solidified/stabilized dye sludge char as a landfill cover material. *J. KSCE J. Civ. Eng.* **2017**, *21*, 2573–2583.
12. He, J.; Guan, J.X.; Zhang, L.; Lü, X.L.; Zhang, C. The effect of dry-wet cycles on microstructure and strength of sludge solidified with soda residue, ground granulated blast furnace slag and quick lime. *J. Adv. Sci. Technol. Water Resour.* **2022**. Available online: <https://kns.cnki.net/kcms/detail/32.1439.TV.20220120.1619.010.html> (accessed on 14 July 2022).
13. Li, Z.X. *Experimental Research on Engineering Properties of Municipal Sludge Solidified with Soda Residue and Ground Granulated Blast Furnace Slag*; Hubei University of Technology: Wuhan, China, 2020.
14. Changjuttaras, K.; Hoy, M.; Horpibulsuk, S.; Rashid, A.S.A.; Horpibulsuk, S.; Arulrajah, A. Solidification and stabilization of metal plating sludge with fly ash geopolymers. *J. Environ. Geotech.* **2019**, 1–10. [[CrossRef](#)]
15. Li, F. *Study of Modified Sewage Sludge Used as Comprehensive Cover Material in MSW Landfill*; Hubei University of Technology: Wuhan, China, 2014.
16. Yi, Y.; Gu, L.; Liu, S. Microstructural and mechanical properties of marine soft clay stabilized by lime-activated ground granulated blastfurnace slag. *Appl. Clay Sci.* **2015**, *103*, 71–76. [[CrossRef](#)]
17. Liu, X.Q.; Yang, Y.H.; Pei, W.B.; Wang, L.; Li, J. Study on Solidification Characteristics of Heavy Metal Contaminated Sludge. *J. Ekoloji* **2018**, *27*, 779–785.
18. Taki, K.; Choudhary, S.; Gupta, S.; Kumar, M. Enhancement of geotechnical properties of municipal sewage sludge for sustainable utilization as engineering construction material. *J. Clean. Prod.* **2020**, *251*, 119723. [[CrossRef](#)]
19. Qian, G.; Cao, Y.; Chui, P.; Tay, J. Utilization of MSWI fly ash for stabilization/solidification of industrial waste sludge. *J. Hazard. Mater.* **2006**, *129*, 274–281. [[CrossRef](#)]
20. Li, Y.L.; Liu, J.W.; Chen, J.Y.; Shi, Y.; Mao, W.; Liu, H.; He, S.; Yang, J.K. Reuse of dewatered sewage sludge conditioned with skeleton builders as landfill cover material. *Int. J. Environ. Sci. Technol.* **2013**, *11*, 233–240. [[CrossRef](#)]
21. Rhew, R.D.; Barlaz, M.A. Effect of Lime-Stabilized Sludge as Landfill Cover on Refuse Decomposition. *J. Environ. Eng.* **1995**, *121*, 499–506. [[CrossRef](#)]
22. Bizarreta, J.; Campos, T. Water Retention Curve and Shrinkage of Sludge from a Leachate Treatment Plant. *J. Unsaturated Soils Res. Appl.* **2012**, 409–414. [[CrossRef](#)]
23. Yang, A.; Yang, S.; Xu, G.; Zhang, W. Study of the Long-Term Deformation Characteristics of Municipal Sludge Solidified Soil under the Coupling Action of Dry-Wet Cycles and Initial Static Deviatoric Stress. *Adv. Civ. Eng.* **2020**, *2020*, 1–15. [[CrossRef](#)]
24. Zhou, Q.; Glasser, F.P. Kinetics and mechanism of the carbonation of ettringite. *Adv. Cem. Res.* **2000**, *12*, 131–136. [[CrossRef](#)]
25. Damidot, D.; Glasser, F.P. Thermodynamic investigation of the CaO-Al₂O₃-CaSO₄-H₂O system at 25 °C and the influence of Na₂O. *J. Cem. Concr. Res.* **1993**, *23*, 221–238. [[CrossRef](#)]
26. Nishikawa, T.; Suzuki, K.; Ito, S.; Sato, K.; Takebe, T. Decomposition of synthesized ettringite by carbonation. *Cem. Concr. Res.* **1992**, *22*, 6–14. [[CrossRef](#)]
27. Zaharaki, D.; Komnitsas, K.; Perdikatsis, V. Use of analytical techniques for identification of inorganic polymer gel composition. *J. Mater. Sci.* **2010**, *45*, 2715–2724. [[CrossRef](#)]